Available online at www.sciencedirect.com
ScienceDirect
Journal of Organometallic Chemistry 693 (2008) 619–624
Journal of Organometallic Chemistry
www.elsevier.com/locate/jorganchem

Synthesis of tungsten compounds with Schiff base ligands prepared from ferrocenecarboxaldehyde: Observation of the migration of an imine double bond

Richard S. Herrick [a,*], Christopher J. Ziegler [b], Melissa Precopio [a], Kerianne Crandall [a], Janet Shaw [b], Ronald M. Jarret [a]

[a] Department of Chemistry, College of the Holy Cross, Worcester, MA 01610, USA
[b] Department of Chemistry, University of Akron, Akron, OH 44325-3601, USA

Received 24 August 2007; accepted 23 November 2007
Available online 4 December 2007

Abstract

The one-pot reactions of ferrocenecarboxaldehyde, $W(CO)_4(pip)_2$ (pip = piperidine) and either 2-(aminomethyl)pyridine or 2-(2-aminoethyl)pyridine lead to clean formation of pyridine imine products $W(CO)_4(\eta^2\text{-}NC_5H_4CH{=}NCH_2C_5H_4FeCp)$ (**1**) and $W(CO)_4(\eta^2\text{-}NC_5H_4C_2H_4N{=}CHC_5H_4FeCp)$ (**2**), respectively. Crystal structures of the two compounds show that in **1** the imine double bond has migrated so that it is conjugated with the pyridine ring while in **2** the imine double bond remains conjugated with the cyclopentadienyl ring. This finding is reinforced by a comparison of dihedral angles in each molecule. IR, NMR and electronic spectra each highlight the differences between the two compounds. Crystal data for $C_{21}H_{16}FeN_2O_4W$ (**1**): monoclinic $P2(1)/c$, $a = 12.768(2)$ Å, $b = 13.593(2)$ Å, $c = 12.981(2)$ Å, $\beta = 119.46°$, $V = 1961.6(4)$ Å^3, $Z = 4$; $C_{22}H_{18}FeN_2O_4W$ (**2**): monoclinic $P2(1)/c$, $a = 16.759(1)$ Å, $b = 8.8612(7)$ Å, $c = 13.802(1)$ Å, $\beta = 95.998(1)°$, $V = 2038.4(3)$ Å^3, $Z = 4$.

Keywords: Crystal structure; Diimine; Ferrocene; Tungsten

1. Introduction

The pyridinecarbaldehyde imine (pyca) ligand is formed by a condensation reaction between pyridine-2-carboxaldehyde and the appropriate amine. This creates an α-diimine that has proven to be a particularly stable ligand in group 6 d^6 carbonyl compounds of the formula $M(CO)_4$-(pyca-R). The stability stems from the favorable back-bonding works better between the metal dπ orbitals and the π^* orbitals of the rigidly planar pyca ligand created by conjugation of the pyridine ring with the exocyclic imine. Complexes created using aromatic amines, aliphatic amines and amino esters and acids have been the focus of several studies [1–8].

We initiated this study to compare the properties of conjugated versus non-conjugated $W(CO)_4$(diimine) complexes. Two non-conjugated diimine ligands with one or two methylene groups separating the pyridine from the imine were targeted. Reflux of either 2-(aminomethyl)pyridine or 2-(2-aminoethyl)pyridine with ferrocenecarboxaldehyde in the presence of $W(CO)_4(pip)_2$ led to two new compounds, $W(CO)_4(\eta^2\text{-}NC_5H_4CH{=}NCH_2\text{-}C_5H_4FeCp)$ (**1**) and $W(CO)_4(\eta^2\text{-}NC_5H_4C_2H_4N{=}CHC_5H_4$ FeCp) (**2**), respectively (see Scheme 1). While the desired compound (**2**), with the ethylene group separating the pyridine from the imine nitrogen was prepared, the corresponding compound with the methylene group separating the pyridine from the imine nitrogen was not obtained. Instead **1**, alternatively formulated as the

* Corresponding author. Fax: +1 508 793 3530.
E-mail address: rherrick@holycross.edu (R.S. Herrick).

0022-328X/$ - see front matter © 2007 Elsevier B.V. All rights reserved.
doi:10.1016/j.jorganchem.2007.11.046

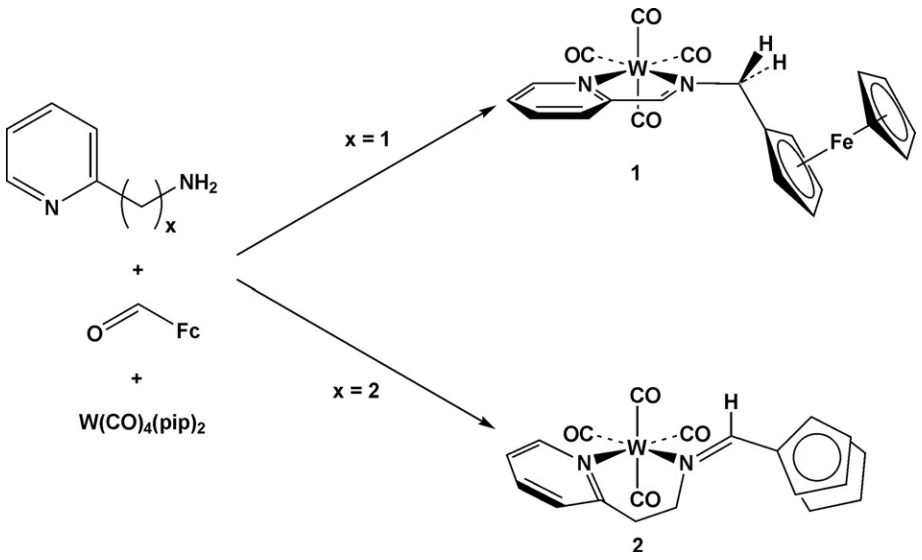

Scheme 1. Reaction scheme for the production of **1** and **2**. Note that **1** and **2** are drawn as their idealized structures in a perspective that highlights key features of the structures and key differences between them.

α-diimine $W(CO)_4$(pyca-$CH_2C_5H_4FeCp$), was obtained as the only product. The reddish-purple color of solutions of **1** and the yellow-orange color of solutions of **2** suggest that there are major differences in these compounds.

A crystal structure of each compound was obtained providing unequivocal proof that the imine bond in **1** has migrated such that it is conjugated with the pyridine ring. Spectroscopic data from infrared, NMR and electronic spectral measurements verify the structural differences of these compounds.

2. Results and discussion

2.1. Syntheses of *1* and *2*

Reflux of one equivalent each of $W(CO)_4(pip)_2$, with a slight excess of ferrocenecarboxaldehyde and 2-(aminomethyl)pyridine in absolute ethanol led to a change in color from light-yellow to dark red. Removal of solvent and purification led to shiny green-black crystals of **1**. A similar procedure using 2-(2-aminoethyl)pyridine as the amine produced a brown solution and a subsequent red solid corresponding to **2** (see Scheme 1). Both reactions proceeded in good yields.

Attempts to prepare these novel ligands in the absence of the tungsten carbonyl fragment were unsuccessful. While some Schiff base compounds containing pyridine are isolable, in many cases they are not [2–6]. Attempts to extend this work preparing Schiff base ligands using ethylenediamine and ferrocenecarboxaldehyde in the presence of $W(CO)_4(pip)_2$ led to insoluble products that could not be analyzed. There have been a few reports of ferrocenyl imines acting as ligands. Diferrocenyldiazabutadiene ligands have been prepared previously and attached to $M(CO)_4$, M = Cr, Mo, W [9]. A 2-pyridyl hydrazone of ferrocenecarboxaldehyde was treated with iron or zinc salts to create the corresponding metal complexes [10]. Recently 6-ferrocenyl-2,2′-bipyridine was prepared and treated with a tungsten precursor to prepare the corresponding $W(CO)_4$(α-diimine) complex [11].

2.2. Crystal structures of *1* and *2*

Crystals of **1** were grown by layering hexane over CH_2Cl_2. The compound crystallizes in the $P2(1)/c$ space group with one molecule in the asymmetric unit. The molecular structure is shown in Fig. 1. Crystal data are given in Table 1 and relevant bond lengths and angles are given in Table 2. Crystals of **2** were grown by layering hexane over CH_2Cl_2. This compound also crystallizes in the $P2(1)/c$ space group with one molecule in the asymmetric unit. The molecular structure is shown in Fig. 2. Crystal data are given in Table 1 and relevant bond lengths and angles are given in Table 2.

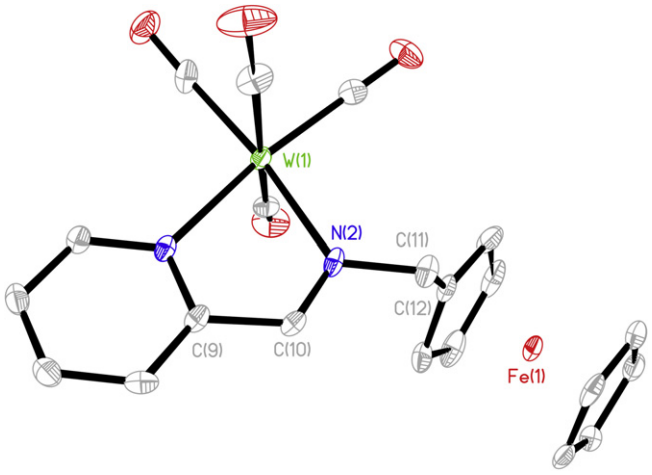

Fig. 1. Molecular structure with 35% thermal ellipsoids for **1**.

Table 1
Crystal data and structure refinement for **1** and **2**

Identification code	**1**	**2**
Empirical formula	$C_{21}H_{16}FeN_2O_4W$	$C_{22}H_{18}FeN_2O_4W$
Formula weight	600.06	614.08
Temperature (K)	100(2)	100(2)
Wavelength (Å)	0.71073	0.71073
Crystal system	Monoclinic	Monoclinic
Space group	*P*2(1)/*c*	*P*2(1)/*c*
Unit cell dimensions		
a (Å)	12.768(2)	16.759(1)
b (Å)	13.593(2)	8.8612(7)
c (Å)	12.981(2)	13.802(1)
α (°)	90	90
β (°)	119.46(1)	95.998(1)
γ (°)	90	90
Volume (Å^3)	1961.6(4)	2038.4(3)
Z	4	4
D_{calc} (Mg/m^3)	2.032	2.001
Absorption coefficient (mm^{-1})	6.630	6.382
F(000)	1152	1184
Crystal size (mm^3)	0.40 × 0.30 × 0.20	0.40 × 0.20 × 0.01
θ Range for data collection (°)	1.83–28.28	1.22–28.31
Index ranges	$-16 \leqslant h \leqslant 16$, $-17 \leqslant k \leqslant 17$, $-17 \leqslant l \leqslant 17$	$-22 \leqslant h \leqslant 22$, $-11 \leqslant k \leqslant 11$, $-17 \leqslant l \leqslant 18$
Reflections collected	17066	17744
Independent reflections [R_{int}]	4692 [0.1116]	4919 [0.0616]
Completeness to θ = 28.28° (%)	96.7	96.8
Absorption correction	SADABS	SADABS
Refinement method	Full-matrix least-squares on F^2	Full-matrix least-squares on F^2
Data/restraints/parameters	4692/0/262	4919/0/271
Goodness-of-fit on F^2	0.993	1.226
Final *R* indices [$I > \sigma(I)$]	$R_1 = 0.0326$, $wR_2 = 0.0771$	$R_1 = 0.0421$, $wR_2 = 0.0903$
R indices (all data)	$R_1 = 0.0380$, $wR_2 = 0.0787$	$R_1 = 0.0540$, $wR_2 = 0.1046$
Largest difference peak and hole (e Å^{-3})	3.418 and −1.429	1.540 and −2.518

Table 2
Bond lengths (Å) and angles (°) for **1** and **2**

1		**2**	
C(1)–W(1)	1.957(5)	C(1)–W(1)	2.012(7)
C(2)–W(1)	2.038(5)	C(2)–W(1)	1.969(6)
C(3)–W(1)	1.968(5)	C(3)–W(1)	2.049(8)
C(4)–W(1)	2.006(5)	C(4)–W(1)	1.939(6)
C(9)–C(10)	1.463(6)	C(9)–C(10)	1.500(8)
C(10)–N(2)	1.280(5)	C(10)–C(11)	1.512(8)
C(11)–N(2)	1.468(6)	C(11)–N(2)	1.481(8)
C(11)–C(12)	1.492(6)	C(12)–N(2)	1.291(8)
N(2)–W(1)	2.212(3)	C(12)–C(13)	1.444(8)
N(1)–W(1)	2.249(4)	N(1)–W(1)	2.267(5)
		N(2)–W(1)	2.256(5)
N(2)–C(10)–C(9)	118.3(4)	C(9)–C(10)–C(11)	112.7(5)
N(1)–C(11)–C(12)	110.8(3)	N(2)–C(11)–C(10)	112.6(5)
C(10)–N(2)–C(11)	116.4(4)	N(2)–C(12)–C(13)	131.9(6)
C(1)–W(1)–C(3)	89.3(2)	C(5)–N(1)–C(9)	118.1(5)
C(1)–W(1)–C(4)	87.0(2)	C(12)–N(2)–C(11)	116.7(5)
C(3)–W(1)–C(4)	82.9(2)	C(4)–W(1)–C(2)	92.4(3)
C(1)–W(1)–C(2)	85.4(2)	C(4)–W(1)–C(1)	89.1(3)
C(3)–W(1)–C(2)	87.6(2)	C(2)–W(1)–C(1)	84.2(3)
C(4)–W(1)–C(2)	167.9(2)	C(4)–W(1)–C(3)	86.0(3)
C(1)–W(1)–N(2)	98.4(2)	C(2)–W(1)–C(3)	81.8(3)
C(3)–W(1)–N(2)	172.0(2)	C(1)–W(1)–C(3)	164.9(3)
C(4)–W(1)–N(2)	95.1(2)	C(4)–W(1)–N(2)	173.0(2)
C(2)–W(1)–N(2)	95.3(2)	C(2)–W(1)–N(2)	94.4(2)
C(1)–W(1)–N(1)	169.9(2)	C(1)–W(1)–N(2)	93.2(2)
C(3)–W(1)–N(1)	99.9(2)	C(3)–W(1)–N(2)	93.4(2)
C(4)–W(1)–N(1)	90.0(2)	C(4)–W(1)–N(1)	93.0(2)
C(2)–W(1)–N(1)	99.0(2)	C(2)–W(1)–N(1)	173.3(2)
N(1)–W(1)–N(2)	72.3(1)	C(1)–W(1)–N(1)	99.9(2)
		C(3)–W(1)–N(1)	94.6(2)
		N(2)–W(1)–N(1)	80.1(2)

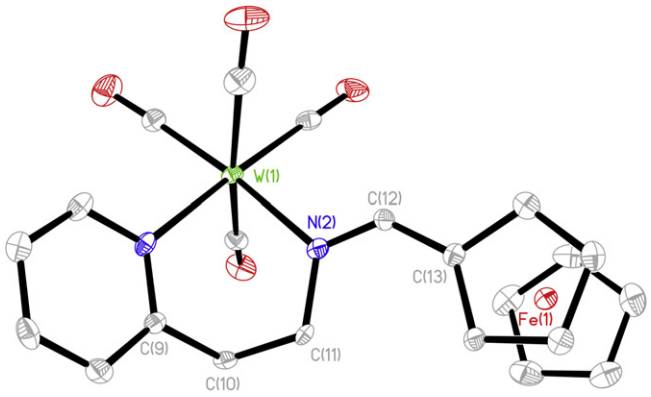

Fig. 2. Molecular structure with 35% thermal ellipsoids for **2**.

Both compounds display a slightly distorted octahedral structure around the tungsten metal center as a consequence of chelate bite angles. The 72.3(1)° bite angle observed for **1** is identical to the value of 72.3(3)° measured for W(CO)$_4$(pyca-β-Ala-Val-OMe) [2]. Compound **2** has a larger bite angle of 80.1(2)° consistent with the six-member ring for the ligand versus the five-member ring found in **1**. The bond distance and bond angle data for **1** clearly shows that the imine double bond has moved inside the metallocycle creating an α-diimine ligand: C(9)–C(10) is 1.46 Å, C(10)–N(2) is 1.28 Å, C(11)–N(2) is 1.47 Å, C(10)–N(2)–C(11) is 116° and N(2)–C(11)–C(12) is 111°. In contrast the bond distance and bond angle data for **2** clearly shows that the imine double bond remains outside the chelate ligand: C(11)–N(2) is 1.48 Å, C(12-)-N(2) is 1.29 Å, N(2)–C(11)–C(10) is 113° and N(2)–C(12)–C(13) is 132°.

A comparison of dihedral angles in the two compounds highlights the features of their bidentate ligands and the key differences between them (see Table 3). The three dihedral angles measured (see Fig. 3) are (a) the angle, α, between the pyridine plane and the plane defined by pyridine ipso carbon, the adjacent carbon C(10) and the next adjacent atom (N(1) for **1** and C(11) for **2**), (b) the angle, β, between the pyridine ring and the plane defined by the mutually *trans* carbonyl carbons and the metal center and, (c) the angle, γ, between the C_5H_4 ring and the plane

Table 3
Comparison of dihedral angles between selected least squares planes for **1** and **2**[a]

Angle	Planes used to measure dihedral angle	**1** (°)	**2** (°)
α	Pyridine ring[b]/ $C_{ipso\text{-}py}$–C–N	2.9	68.9
β	Pyridine ring[b]/C–W–C (trans COs)	84.3	41.8
γ	C_5H_4R ring[c]/$C_{ipso\text{-}py}$–C–$N_{exocyclic\ imine}$	63.7	2.7

[a] Error on the angles are less than or equal to 0.5 degrees. Least squares planes and dihedral angles calculated from crystal data using Mercury version 1.4. Copyright CCDC 2001–2005. http://www.ccdc.cam.ac.uk/mercury/.
[b] Defined by the nitrogen atom and five carbon atoms in the ring.
[c] Defined by the five carbon atoms in the ring.

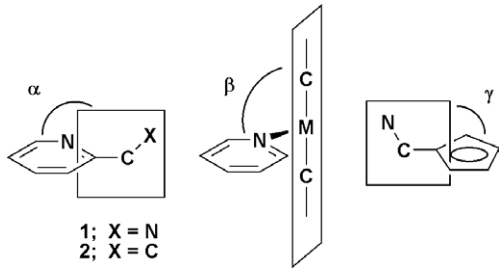

Fig. 3. Drawings depicting the measurement of the dihedral angles mentioned in the text.

defined by the C_5H_4 ipso carbon, the adjacent carbon and the exocyclic imine nitrogen. Angle α, which should be near 0° for there to be conjugation between the pyriding ring and an exocyclic imine, is 2.9° for **1** and 68.9° for **2**. Similarly angle β, measures the alignment of the pyridine ring with the $W(CO)_4$ fragment and should be near 90° for maximal backbonding from the metal to the pyridine and imine nitrogens. The angle is 84.3° for **1** and 41.8° for **2**. This shows that the pyca ligand in **1** is aligned for maximal backbonding from the $W(CO)_4$ fragment and that the pyridine ring in **2** has to twist to create the six-member chelate ring. Angle γ, measures the twisting away from co-planarity between the plane of the C_5H_4 ring and the plane formed by the ipso Cp carbon, the carbon bound to the ring and the imine nitrogen. Compound **2** shows a very small distortion with a 2.7° angle showing that C(12)–N(2) double bond lies nearly in the same plane as the C_5H_4 ring to gain the effects of conjugation with the ring. The 63.7° angle observed for **1** shows that there is no need for co-planarity since the imine bond has moved to the other side of the nitrogen creating the pyca ligand. The ferrocenyl group in each molecule is unexceptional with the rings adopting an eclipsed conformation.

2.3. Spectroscopic characterization

IR spectra for the two compounds recorded in CH_2Cl_2 displayed the expected pattern for a *cis*-substituted tetracarbonyl. Each band for **2** is about 15–20 cm^{-1} lower indicating greater backbonding to the carbonyls in that compound. This indicates the chelating ligand in **2** is less efficient at backbonding than the pyca ligand in **1**.

In the ^{13}C NMR spectra of each compound the two mutually *trans* carbonyls in each compound appear as a single resonance. Ferrocenyl rotation around the C–N single bond in **1** leads to a mirror plane accounting for the equivalence of the trans COs. For **2**, a waggling of the chelate ligand would equilibrate the two *trans* CO ligands. The peaks for the imine proton and carbon for **1** appear at 8.57 and 161.8 ppm, shifted upfield from the corresponding peaks for **2** observed at 8.84 and 172.2 ppm, respectively [10].

The two compounds have dramatically different appearances that are verified by electronic spectroscopy. Compound **1** is isolated as large lustrous green-black crystals and forms dark red or reddish-purple solutions in methanol and toluene, respectively. In each solvent **2** produces a yellow solution. In methanol the main feature in the electronic spectrum of **1** (see Fig. 4) is a band centered at 516 nm ($\varepsilon = 8700\ M^{-1}\ cm^{-1}$). This band is assigned to a primarily metal-to-ligand charge-transfer (MLCT) transition based on the similarity to previous pyca compounds [6,12–14]. In toluene the band is red-shifted to 546 nm ($\varepsilon = 7600\ M^{-1}\ cm^{-1}$) due to the negative solvatochromic effect observed for charge-transfer compounds of this type [6]. The value Δ, defined as the difference in energy for the band in different solvents is 1064 cm^{-1}, similar to values observed previously [6]. Compound **1** also displays a band at 359 nm ($\varepsilon = 3100\ M^{-1}\ cm^{-1}$) in methanol likely due to a d–d transition. In agreement with this assignment is the fact that this band has essentially no solvent dependence. As seen for similar α-diimine group 6 tetracarbonyl compounds the extinction coefficient is larger than expected for a ligand field based transition. The principal feature in the electronic spectrum of **2** (Fig. 4) in methanol is a band at 352 nm ($\varepsilon = 7700\ M^{-1}\ cm^{-1}$). The pyridine and imine are not conjugated in this compound so their transitions occur at higher energy as observed for compounds such as $Mo(CO)_4(py)_2$ [15]. Assignment of the band primarily to an MLCT transition is supported by its negative solvatochromatic shift in toluene to 376 nm methanol ($\varepsilon = 9200\ M^{-1}\ cm^{-1}$, $\Delta = 1813\ cm^{-1}$). Compound **2** also displays a slight shoulder in its spectrum at around 460 nm attributed to the ferrocene chromophore.

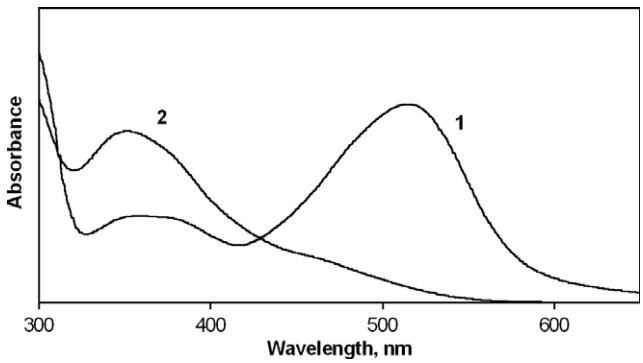

Fig. 4. Electronic spectrum of **1** and **2** in methanol.

2.4. Conclusion

This study was undertaken with the goal of preparing two new related compounds with a non-conjugated diimine bound to a $W(CO)_4$ fragment. This goal was only partly realized. When the diimine created using 2-(2-aminoethyl)pyridine was attached to the $W(CO)_4$ fragment the predicted compound, **2**, was obtained. The ligand in this compound has two methylene carbons separating the pyridine ring from the imine nitrogen. When the diimine created using 2-(aminomethyl)pyridine was attached to the $W(CO)_4$ fragment, compound **1** was obtained. This molecule shows an unexpected migration of the imine bond creating a pyca chelate ligand. It is presumed that the reason for this migration is the formation of the stable pyca ligand. This ligand has conjugation of the imine bond with the pyridine ring and also strong backbonding from the $W(CO)_4$ fragment into the π^* orbitals of each nitrogen. While migration does cause it to lose the conjugation between the C_5H_4 ring and the imine, this is apparently more than made up by the combination of the two stabilizations that result. Characterization by various types of spectroscopy showed that significant differences exist between the two compounds. The crystal structures of the compounds are also quite different with a near planar pyca ligand for **1** that promotes a strong backbonding interaction. Ligand **2** adopts a twisted conformation, which weakens the interaction.

3. Experimental details

3.1. Spectroscopic measurements

NMR spectra were recorded on a Oxford NMR AS400 spectrometer. IR spectra were recorded on a Perkin–Elmer Spectrum One FT-IR spectrometer, while electronic spectra were obtained from a Cary 50 Scan UV–Vis spectrometer. Elemental analyses were performed by Atlantic Microlab of Norcross, GA 30091.

3.2. Materials

Starting materials for syntheses were obtained from commercial sources and used without further purification. Solvents were degassed prior to use and preparations were performed under a nitrogen atmosphere. $W(CO)_4(pip)_2$ (pip = piperidine) [16] was prepared using the literature procedures.

3.3. Synthesis of *1*

Ferrocenecarboxaldehyde (2.80 mmol), 2-(aminomethyl)pyridine (2.80 mmol) and $W(CO)_4(pip)_2$ (2.30 mmol) were added to 25 mL of absolute ethanol. The solution was warmed to reflux. The solution color changed from orange to dark red. After 3 h the solvent was removed by rotary evaporator. The residue was dissolved in a minimum amount of CH_2Cl_2 and hexane was layered over it. The next day **1** was isolated as green/black crystals. The collected crystals were recrystallized a second time and isolated in 58% yield.

Compound **1**. IR (CH_2Cl_2): 2008 (s), 1897 (vs), 1878 (sh), 1833 (s) cm^{-1}. Anal. Calc. for $C_{21}H_{16}N_2O_4WFe$: C, 42.03; H, 2.69; N, 4.67. Found: C, 41.91; H, 2.67; N, 4.67%. ^1H NMR (d_6-DMSO): δ 9.19 (d, $^3J = 5.2$ Hz, 1H, *H* on py), 8.57 (s, 1H, N=C*H*), 7.85 (m, 1H, *H* on py), 7.70 (d, $^3J = 5.6$ Hz, 1H, *H* on py), 7.32 (m, 1H, *H* on py), 5.19 (s, 2H, CH_2), 4.35 (br s, 2H, *H* on C_5H_4), 4.28 (br s, 2H, *H* on C_5H_4), 4.25 (s, 5H, Cp). ^{13}C NMR (d_6-DMSO): δ 217.4 (CO_{cis}), 215.8 (CO_{cis}), 198.6 (CO_{trans}), 161.8 (*C*=N), 155.7 (*C* on py), 153.0 (*C* on py), 136.6 (*C* on py), 127.6 (*C* on py), 126.5 (*C* on py), 82.2 CH_2, 70.0 (ipso *C* on Cp), 69.5 (*C* on C_5H_4), 69.2 (*C* on C_5H_4), 65.1 (C_5H_5). UV–Vis, λ_{max}, nm (ε, $M^{-1}\,cm^{-1}$). MeOH: 516 (8700), 359 (3100). Toluene: 546 (7600), 362 (3000). M.p. 195 °C.

3.4. Synthesis of *2*

Ferrocenecarboxaldehyde (2.80 mmol), 2-(2-aminoethyl)pyridine (2.80 mmol) and $W(CO)_4(pip)_2$ (2.30 mmol) were added to 25 mL of absolute ethanol. The solution was warmed to reflux. The solution color changed from orange to brown. After 3 h the solvent was removed by rotary evaporator. The residue was dissolved in a minimum amount of CH_2Cl_2 and hexane was layered over it. The next day **2** was isolated as a red solid. The collected crystals were recrystallized a second time and isolated in 91% yield.

Compound **2**. IR (CH_2Cl_2): 1993 (s), 1842 (s), 1811 (vs) cm^{-1}. Anal. Calc. for $C_{22}H_{18}N_2O_4WFe$: C, 43.03; H, 2.95; N, 4.56. Found: C, 42.75; H, 2.97; N, 4.54%. ^1H NMR (d_6-DMSO): δ 9.20 (d, $^3J = 5.6$ Hz, 1H, *H* on py), 8.84 (s, 1H, N=CH), 7.76 (m, 1H, *H* on py), 7.35 (d, $^3J = 3.6$ Hz, 1H, *H* on py), 7.15 (m, 1H, *H* on py), 4.59 (s, 4H, C_5H_4), 4.28 (s, C_5H_5), 3.57 (m, 2H, CH_2), 3.37 (m, 2H, CH_2) ^{13}C NMR (d_6-DMSO): δ 220.6 (CO_{cis}), 218.7 (CO_{cis}) 205.5 (CO_{trans}), 172.2 (*C*=N), 162.3 (*C* on py), 155.7 (*C* on py), 140.0 (*C* on py), 126.9 (*C* on py), 127.8 (*C* on py), 74.58, (ipso *C* on Cp) 74.0 (*C* on C_5H_4), 73.7 (*C* on C_5H_4), 70.3 (C_5H_5), 52.2 (CH_2), one CH_2 peak obscured by solvent. UV–Vis, λ_{max}, nm (ε, $M^{-1}\,cm^{-1}$). MeOH: 352 (7700). Toluene: 376 (9200). M.p. 192 °C.

3.5. X-ray structure determination of *1* and *2*

Crystals for crystallographic analysis were mounted on a cryoloop using Paraton N-Exxon oil and placed under a stream of cold nitrogen gas. Analyses of the data sets showed negligible decay during data collection. The data were corrected for absorption using the SADABS program. The structures were refined using the Bruker SHELXTL Software Package (Version 6.10) and were solved until the final anisotropic full-matrix, least squares refinement of F^2 converged [17]. Hydrogen atoms were assigned ideal positions and refined isotropically. Additional experimental details are provided in Table 1.

Acknowledgements

K.C. thanks the Simeon J. Fortin Charitable trust for a summer fellowship. R.S.H. thanks Holy Cross for research support and the National Science Foundation for funds to purchase the NMR facilities (CHE-0079348). R.S.H. and C.J.Z. acknowledge a Supplementary Grant from the Petroleum Research Foundation (PRF# 39625-G5M). We also wish to acknowledge NSF Grant CHE-0116041 for funds used to purchase the Bruker-Nonius diffractometer. The authors thank Prof. Tim Brunker for helpful discussions.

Appendix A. Supplementary material

CCDC 657038 and 657039 contain the supplementary crystallographic data for this paper. These data can be obtained free of charge from The Cambridge Crystallographic Data Centre via www.ccdc.cam.ac.uk/data_request/cif. Supplementary data associated with this article can be found, in the online version, at doi:10.1016/j.jorganchem.2007.11.046.

References

[1] L. Chan, A.J. Lees, J. Chem. Soc., Dalton Trans. (1987) 513–517.
[2] R.S. Herrick, J. Dupont, I. Wrona, J. Pilloni, M. Beaver, M. Benotti, F. Powers, C.J. Ziegler, J. Organomet. Chem. 692 (2007) 1226–1233.
[3] T. Ederer, R.S. Herrick, W. Beck, Z. Anorg. Allg. Chem. 633 (2007) 235–238.
[4] R.S. Herrick, I. Wrona, N. McMicken, G. Jones, C.J. Ziegler, J. Shaw, J. Organomet. Chem. 689 (2004) 4848–4855.
[5] R.S. Herrick, C.J. Ziegler, H. Bohan, M. Corey, M. Eskander, J. Giguere, N. McMicken, I.E. Wrona, J. Organomet. Chem. 687 (2003) 178–184.
[6] R.S. Herrick, K.L. Houde, J.S. McDowell, L.P. Kiczek, G. Bonavia, J. Organomet. Chem. 589 (1999) 29–37.
[7] R. Garcia-Rodriguez, D. Miguel, Dalton Trans. (2006) 1218–1225.
[8] H. Brunner, W.A. Herrmann, Chem. Ber. 105 (1972) 770–783.
[9] B. Bildstein, M. Malaun, H. Kopacka, M. Fontani, P. Zanello, Inorg. Chim. Acta 300–302 (2000) 16–22.
[10] J. Silver, G.R. Fern, J.R. Miller, E. Slade, M. Ahmet, A. Houlton, D.J. Evans, G.J. Leigh, J. Organomet. Chem. 637–639 (2001) 311–317.
[11] P. Edinc, A.M. Oenal, S. Oezkar, J. Organomet. Chem. 692 (2007) 1983–1989.
[12] R.W. Balk, T. Snoeck, D.J. Stufkens, A. Oskam, Inorg. Chem. 19 (1980) 3015–3021.
[13] P.C. Servaas, H.K. Van Dijk, T.L. Snoeck, D.J. Stufkens, A. Oskam, Inorg. Chem. 24 (1985) 4494–4498.
[14] A.J. Lees, Chem. Rev. 87 (1987) 711–743.
[15] M.S. Wrighton, D.L. Morse, J. Organomet. Chem. 97 (1975) 405–419.
[16] D.J. Darensbourg, R.L. Kump, Inorg. Chem. 17 (1978) 2680–2682.
[17] G.M. Sheldrick, SHELXTL, Crystallographic Software Package, Version 6.10, Bruker-AXS, Madison, WI, 2000.